PERGAMON

Building and Environment 34 (1999) 245–251

BUILDING AND ENVIRONMENT

Mixing characteristics in a ventilated room with non-isothermal ceiling air supply

H. Xue*, C. Shu

Department of Mechanical and Production Engineering, National University of Singapore, 10 Kent Ridge Crescent, Singapore 119260

Received 16 September 1997; accepted in revised form 17 April 1998

Abstract

A two-dimensional turbulence k–ε model is used to predict distribution of air velocity, temperature and turbulence kinetic energy in an air-conditioned room using ceiling air supply. Mixing characteristics of the airflow are analyzed under different air supply velocities and temperatures. A modified Archimedes number is correlated with the parameters characterizing heat transfer, ventilation system, and turbulence kinetic energy of room air flow. Significant correlations have been shown. It is found that the linear ceiling air supply air-conditioning system with a high level return air provides excellent air mixing across a wide range of Archimedes numbers. The results are useful for air-conditioning design and thermal comfort study. © 1998 Elsevier Science Ltd. All rights reserved.

Nomenclature

A cross section area
Ar modified Archimedes number ($=Gr/Re^{2.5}$)
B width of room
C_μ, C_1, C_2, C_3 turbulent constants
D_h hydraulic diameter of room
g gravitational acceleration
G_B buoyancy production term
G_k shear production term
Gr Grashof number $\left(=\dfrac{gD_h^3\Delta T_0/T_m}{\nu^2}\right)$
H height of room
k turbulent kinetic energy
k_a average turbulent kinetic energy
Nu local Nusselt number
$\overline{Nu}$ average Nusselt number
P pressure
Pr Prandtl number
Re Reynolds number $\left(=\dfrac{D_h U_r}{\nu}\right)$
T temperature
T_m mean room temperature
T_w wall temperature
U_r equivalent room velocity
u, v mean velocity components
u_τ friction velocity
V volumetric flow rate
W length of room
x, y Cartesian coordinates
y^+ dimensionless distance from wall ($=uy/\nu$)

Greek symbols
ε turbulence dissipation rate
λ thermal conductivity
μ molecular viscosity
μ_t eddy viscosity
ν_t turbulent dynamic viscosity
σ_T turbulent Prandtl number
σ_k, σ_ε turbulent Schmidt number
Γ exchange coefficient

Subscripts
e at air exhaust duct
eff effective
l at left wall
r at right wall
0 at air supply inlet

1. Introduction

Understanding the indoor air distribution characteristics is essential to the design of a ventilation system and the control of room thermal and air quality conditions. Ceiling air supply is one of the most widely used ventilation and air conditioning methods in the region. This method requires that the supply air and

* Corresponding author. Tel.: 0065 874 6479; fax: 0065 779 1459; e-mail: mpexueh@nus.edu.sg

S0360-1323/99 $—see front matter
PII: S0360-1323(98)00015-8

room air are mixed well by the interactions of the supply jet momentum and buoyancy. The supply air is functioned to dilute the concentration of contaminants in the room. Because the non-isothermal air is supplied at high level, the concentration levels above the occupied zone are generally lower than those existing within the zone, which results in an overall relative ventilation efficiency of less than one. In addition, stagnant zones of high concentration levels and short circulating of supply air to the extract points can cause a sharp drop in the ventilation efficiency. To avoid these occurrences, it is important to carry out an accurate prediction on the air mixing characteristics during design stage.

The prediction of air movement in rooms by computational fluid dynamic (CFD) method started in the 1970s [1]. With rapid increase of computer power, the topic has attracted more and more attention [2, 3, 4]. ASHRAE technical meeting now regularly includes technical sessions on CFD developments and application to room air motion studies. However, numerical studies on air mixing characteristics of ceiling air supply configuration are few to date. In addition, the available overwhelming majority of contributions are from the United States and Europe. While these areas certainly cover a broad range in the climatic spectrum, the research of room air distribution under the equatorial climate is grossly underpresented in the literature.

The present study simulates the air motion in an air-conditioned room with ceiling air supply. The main purpose is to investigate the effects of important parameters such as Archimedes number on air velocity and temperature distribution, ventilation efficiency, heat transfer and turbulent mixing. As a preliminary step, the effluence of room partitions, furnishings as well as internal heat source are not considered so that the basic mixing characteristics of air can be examined carefully.

2. Mathematical model

During the last two decades, a number of numerical models have been compiled for the prediction of room air motion. Besides the k–ε model, engineers in this field have begun applying more sophisticated models, such as algebraic and Reynolds stress models. Using ad-hoc modifications on the standard k–ε model to improve the computed results is also a common practice. However, a recent study by Chen [5, 6] showed that, in simulating air flow in rooms, the standard k–ε model gives stable and good results across all the cases. The standard k–ε model is therefore used for the present study.

With reference to Fig. 1, steady, turbulent flow and heat transfer are considered within a rectangular room that is supplied with cooled air from a linear ceiling slot. The room has an exhaust outlet at the up-right wall. The linear ceiling air supply configuration enables us

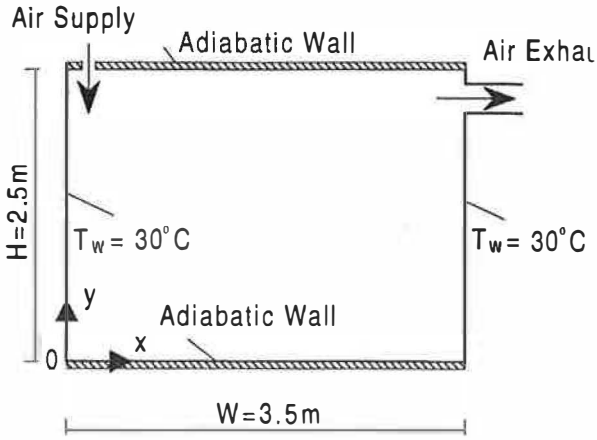

Fig. 1. Schematics of simulated room.

to simplify the numerical simulation by using a tw dimensional mathematical model. Assuming that t fluid is incompressible and that the Boussinesq appro mation is valid, and employing the eddy viscos concept, which assumes that the turbulent stresses a proportional to the mean velocity gradients, the tim averaged continuity, momentum and energy equatio are written as

$$\frac{\partial u}{\partial x}+\frac{\partial v}{\partial y}=0$$

$$\rho u\frac{\partial u}{\partial x}+\rho v\frac{\partial u}{\partial y}=-\frac{\partial P}{\partial x}+2\frac{\partial}{\partial x}\left(\mu_{eff}\frac{\partial u}{\partial x}\right)+\frac{\partial}{\partial y}\left(\mu_{eff}\frac{\partial u}{\partial y}\right)+\frac{\partial}{\partial y}\left(\mu_{eff}\frac{\partial v}{\partial x}\right)$$

$$\rho u\frac{\partial v}{\partial x}+\rho v\frac{\partial v}{\partial y}=-\frac{\partial P}{\partial y}+\frac{\partial}{\partial x}\left(\mu_{eff}\frac{\partial v}{\partial x}\right)+2\frac{\partial}{\partial y}\left(\mu_{eff}\frac{\partial v}{\partial y}\right)+\frac{\partial}{\partial x}\left(\mu_{eff}\frac{\partial u}{\partial y}\right)+\rho g\beta(T-T_i)$$

$$\rho u\frac{\partial T}{\partial x}+\rho v\frac{\partial T}{\partial y}=\frac{\partial}{\partial x}\left(\Gamma_{eff}\frac{\partial T}{\partial x}\right)+\frac{\partial}{\partial y}\left(\Gamma_{eff}\frac{\partial T}{\partial y}\right)$$

where the pressure term in the momentum equations actually a pseudo-pressure. μ_{eff} is combined laminar a turbulent stresses and Γ_{eff} is effective exchange coefficie They are given by

$$\mu_{eff}=\mu+\mu_t$$

$$\Gamma_{eff,T}=\frac{\mu}{Pr}+\frac{\mu_t}{\sigma_t}$$

where Pr and σ_t are the laminar and turbulent Pran numbers respectively. The eddy viscosity is obtained the Prandtl–Kolmogorov relation,

$$\mu_t = \rho C_\mu \frac{k^2}{\varepsilon} \tag{7}$$

C_μ being empirically determined coefficient.

The turbulent kinetic energy and dissipation transport equations for buoyant flows can be written as follows.

$$\rho u \frac{\partial k}{\partial x} + \rho v \frac{\partial k}{\partial y} = \frac{\partial}{\partial x}\left(\Gamma_{eff,k} \frac{\partial k}{\partial x}\right) + \frac{\partial}{\partial y}\left(\Gamma_{eff,k} \frac{\partial k}{\partial y}\right) + G_k + G_B - \rho\varepsilon \tag{8}$$

$$\rho u \frac{\partial \varepsilon}{\partial x} + \rho v \frac{\partial \varepsilon}{\partial y} = \frac{\partial}{\partial x}\left(\Gamma_{eff,\varepsilon} \frac{\partial \varepsilon}{\partial x}\right) + \frac{\partial}{\partial y}\left(\Gamma_{eff,\varepsilon} \frac{\partial \varepsilon}{\partial y}\right) + C_1 \frac{\varepsilon}{k}(G_k + G_B)(1 + C_3 R_f) - C_2 \frac{\rho\varepsilon^2}{k} \tag{9}$$

where

$$\Gamma_{eff,k} = \mu + \frac{\mu_t}{\sigma_k}, \quad \Gamma_{eff,\varepsilon} = \mu + \frac{\mu_t}{\sigma_\varepsilon}$$

$$G_k = \left[2\left(\frac{\partial u}{\partial x}\right)^2 + 2\left(\frac{\partial v}{\partial y}\right)^2 + \left(\frac{\partial u}{\partial y} + \frac{\partial v}{\partial x}\right)^2\right] \tag{10}$$

$$G_B = -\beta g \frac{\mu_t}{\sigma_t} \frac{\partial T}{\partial y} \tag{11}$$

In the above equations, G_B represents an exchange between the turbulent kinetic energy and the potential energy. The constant C_3 controls the effect of buoyancy on the ε equation. Rodi [7] suggested that flux Richardson number can be defined as

$$R_f = -\frac{G_B}{G_k + G_B} \tag{12}$$

for horizontal shear layers and $R_f = 0$ for vertical shear layers. The empirical constants C_1, C_2, C_3, C_μ, σ_k and σ_ε are adopted from Rodi [7] and are given herein: $C_1 = 1.44$; $C_2 = 1.92$; $C_3 = 0.8$; $C_\mu = 0.09$; $\sigma_k = 1.0$ and $\sigma_\varepsilon = 1.3$.

All the physical properties in above equations are calculated at reference temperature 30 C.

Referring to Fig. 1, the ceiling and floor are considered as adiabatic walls which lead to a no-flux boundary condition for the temperature. The surrounding walls are considered isothermal at the environmental temperature (30 C). At the low-turbulence region close to the walls, the form of the wall-function approach has been chosen such that the standard logarithmic velocity and temperature profiles are assumed to hold between the solid wall and the first grid point next to it. By assuming local equilibrium, the kinetic energy of turbulence and the dissipation rate can be decided. The formation and implementation of these wall functions is standard [7]. The wall functions are valid for forced convection flow with small pressure gradients and for $y^+ > 10.8$. Since the friction velocity can be expressed as

$$u_\tau = \sqrt{\nu\left(\frac{\partial u}{\partial y}\right)_w} = \sqrt{\nu \frac{|u|}{y}} \tag{13}$$

where y is the distance between the wall and first grid point, the constraint for y^+ requires a corresponding local Reynolds number $|u|y/\nu$ to be larger than 117. For the near wall grid points where $|u|y/\nu \leqslant 117$, laminar flow calculation will be carried out locally.

At the inlet, all dependent variables are prescribed. A uniform vertical velocity and temperature are assumed. The values of k and ε are empirically given as $k_0 = 0.02 v_0^2$ and $\varepsilon_0 = C_\mu k_0^{1.5}/0.05$.

At the outlet, a five-grid-long (0.5 m) extension is added into the exhaust duct to facilitate boundary condition specifications that do not compromise local flow field accuracy. Zero-gradient conditions are prescribed at the end of the extension for all dependent variables.

The partial differential equations governing turbulent mixed convection are reduced to systems of simultaneous equations by a control-volume based, finite-difference procedure where the velocity control volumes are staggered with respect to the main control volumes. The resulting algebraic equations are solved iteratively using a line-by-line TDMA solution procedure and the SIMPLE algorithm described by Patankar [8]. Steady-state solutions are obtained using underrelaxation techniques.

To decide whether a solution is converged, the ratio of the residual mass source to the maximum mass flux across a control surface is set to be less than 0.1%. A general convergence is then usually satisfied after 6000 iterations. The computations are performed on 42×27 grids. The solution procedure has been validated against the benchmark results of de Vahl Davis [9] for laminar natural convection in an enclosure with aspect ratio of 1, with excellent agreement having been obtained.

3. Numerical experiments

As illustrated in Fig. 1, numerical experiments assumed that the non-isothermal air is supplied from a linear ceiling slot vertically down to the room at flow rates ranging between 0.2 m/s and 0.8 m/s, which is approximately equivalent to 8 and 33 air changes per hour (ACH). The supply air temperatures are calculated from 288–302 K.

Archimedes number ($Ar = Gr/Re^2$) is conventionally quoted as a non-dimensional number in building service engineering to characterize non-isothermal room ventilation flows. It represents the ratio of thermal buoyancy force to inertial force. However, a recent report by Zhang et al. [10] showed that the Archimedes number defined as above is not the dominant parameter for the phenomena

and the effect of Re number still needs to be accounted for. Zhang et al. [10] also demonstrated that a possible compromise is to take a new scaling factor between Ar number similarity and Re number similarity, which is implicitly to weight more on the exponent of Re number defined in Ar number. But it is difficult to quantify the exponent. Based on the study of the fire-induced temperature stratification in a ventilated tunnel [11], we propose that in the study of room air motion, Archimedes number might be defined as

$$Ar = \frac{Gr}{Re^{2.5}} \tag{14}$$

where

$$Gr = \frac{gD_h^3 \Delta T_0 / T_m}{\nu^2} \tag{15}$$

$$Re = \frac{D_h U_r}{\nu} \tag{16}$$

$D_h = 2BH/(B+H)$ is hydraulic diameter of room, $U_r = V/(BH)$ is equivalent room velocity, V is volumetric flow rate, $T_m = 0.5\,(T_0 + T_w)$ is mean room temperature, T_0 is supply air temperature and T_w is wall temperature, $\Delta T_0 = T_w - T_0$.

Due to the buoyancy forces aiding or opposing the imposed supply airflow, the left and right side walls in the room experiences different circumstances in mixed convection. The average Nusselt numbers for two side vertical walls are defined separately as

$$\overline{Nu_l} = \frac{1}{H}\int_H Nu_l dy = \frac{1}{H}\int_H \frac{H}{\lambda(T_w - T_e)}\left(-\lambda\frac{\partial T}{\partial x}\right)_{x=0} dy \tag{17}$$

$$\overline{Nu_r} = \frac{1}{H}\int_H Nu_l dy = \frac{1}{H}\int_H \frac{H}{\lambda(T_w - T_e)}\left(-\lambda\frac{\partial T}{\partial x}\right)_{x=w} dy \tag{18}$$

where T_e is the mixed exhaust temperature at the air exhaust outlet. T_e characterizes the average thermal energy state of the fluid at the exhaust duct and is calculated by

$$T_e = \frac{1}{A_e u_e}\int_{A_e} uT dA_e \tag{19}$$

The numerical experiment conditions are summarized in Table 1.

4. Results and discussion

The supply airflow is modestly turbulent, and the room flow would be low turbulent. With insulated ceiling and floor, heat transfer is limited to the vertical walls. The geometry of air supply and exhaust is characterized by a thermal boundary layer of cool fluid forming on warm walls. A forced air circulation loop is formed. The boundary layers interact and the center of the room remains nearly stagnant.

Figure 2 displays steady state velocity solutions at different Ar numbers. Figures 2(a), (b) and (c) with the temp. difference $T_w - T_0 = 1$ C, simulates a pure ventilation situation, while Fig. 2(g), (h) and (i) with $T_w - T_0 = 15$ C, represents a strong air-conditioned case. A supply air temperature decreases, the velocity components increase due to larger buoyancy force, but the flow circulation pattern remains almost unchanged. Even for the case with the highest Ar number (Fig. 2(g)), there is no flow separation at the left side wall where opposing flow is formed.

In Fig. 3, isotherms are plotted for the different Ar numbers. The air temperature in the room is evenly distributed. The temperature gradients are restricted within a thin layer close to the walls except at the region near the left floor corner of the room, where the slow air movement causes insufficient air mixing. The results show that the ceiling supply exhibits very effective air mixing characteristics even when the supplying air velocity is as low as 0.2 m/s. The average room temperature is only slightly reduced with the increase of supplying air velocity which reflects the room air change rate.

The average Nusselt numbers for both walls are shown in Figs 4 and 5 to demonstrate the heat transfer through the vertical walls. Generally, the heat transfer in aiding flow circumstance is more significant than that in opposing flow. Because of the location of air supply, the left side wall is imposed by a cooler air flow and larger initial velocity. As a result, the average Nusselt number at the left side wall is higher than that at the right side. It is interesting to note that the Nusselt numbers are little affected by Ar and Re numbers. Mullejans studied the room air movement with the air supplied from a wall at high level [12]. He defined the averaged Nusselt number using $(T_w - T_0)$ as reference temperature difference. The results showed that the averaged Nusselt number is a

Table 1
Numerical experimental conditions

No.	u_0	T_0	T_w	Re	Gr	Ar
1	0.2 m s	288 K ~ 302 K	303 K	714	3.14×10^8 ~ 5.67×10^9	23 ~ 416
2	0.4 m s	288 K ~ 302 K	303 K	1429	3.14×10^8 ~ 5.67×10^9	4.1 ~ 73
3	0.8 m/s	288 K ~ 302 K	303 K	2857	3.14×10^8 ~ 5.67×10^9	0.7 ~ 13

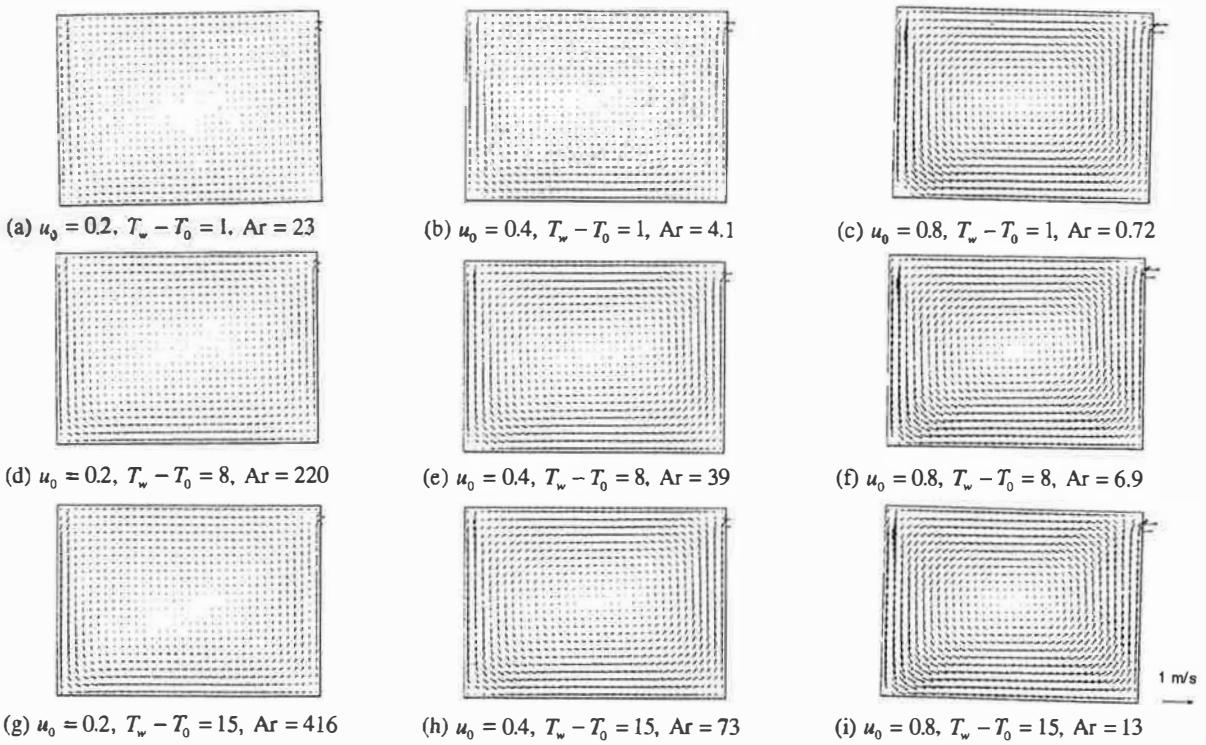

(a) $u_0 = 0.2$, $T_w - T_0 = 1$, Ar = 23 (b) $u_0 = 0.4$, $T_w - T_0 = 1$, Ar = 4.1 (c) $u_0 = 0.8$, $T_w - T_0 = 1$, Ar = 0.72

(d) $u_0 = 0.2$, $T_w - T_0 = 8$, Ar = 220 (e) $u_0 = 0.4$, $T_w - T_0 = 8$, Ar = 39 (f) $u_0 = 0.8$, $T_w - T_0 = 8$, Ar = 6.9

(g) $u_0 = 0.2$, $T_w - T_0 = 15$, Ar = 416 (h) $u_0 = 0.4$, $T_w - T_0 = 15$, Ar = 73 (i) $u_0 = 0.8$, $T_w - T_0 = 15$, Ar = 13

Fig. 2. Predicted velocity vectors.

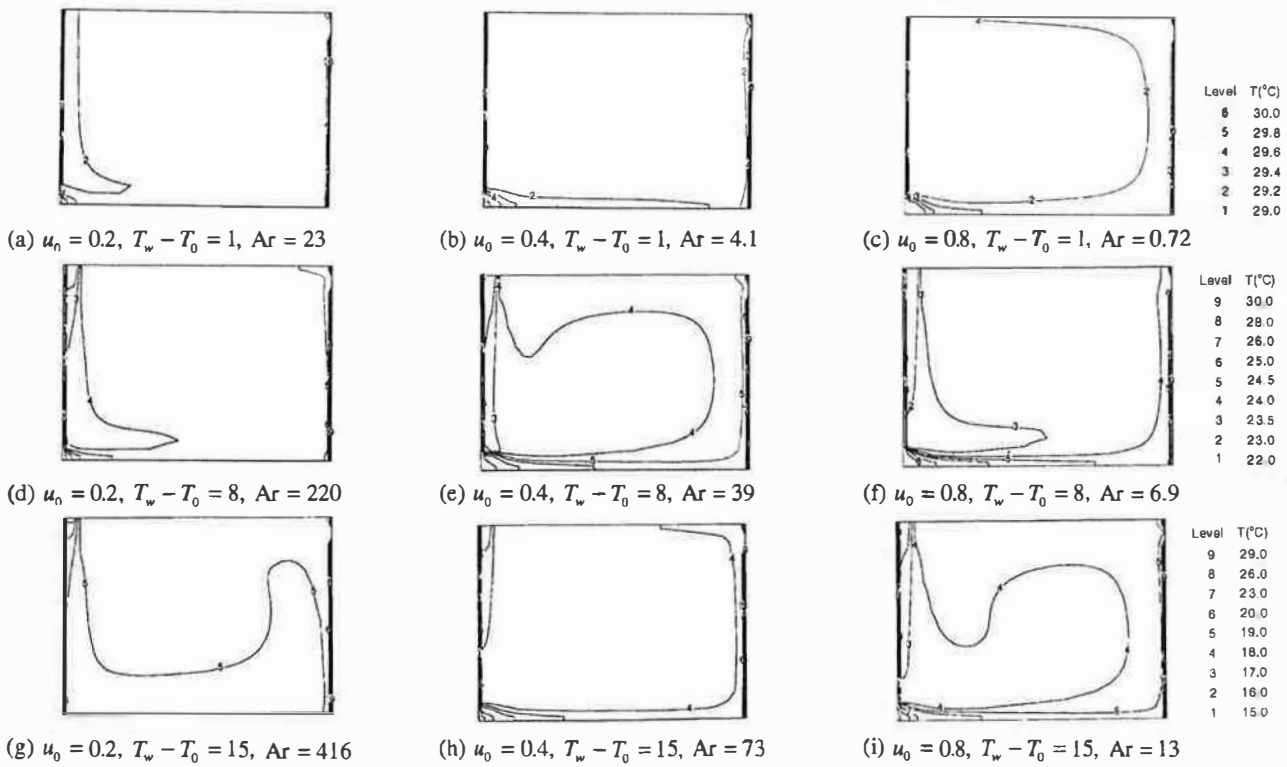

(a) $u_0 = 0.2$, $T_w - T_0 = 1$, Ar = 23 (b) $u_0 = 0.4$, $T_w - T_0 = 1$, Ar = 4.1 (c) $u_0 = 0.8$, $T_w - T_0 = 1$, Ar = 0.72

(d) $u_0 = 0.2$, $T_w - T_0 = 8$, Ar = 220 (e) $u_0 = 0.4$, $T_w - T_0 = 8$, Ar = 39 (f) $u_0 = 0.8$, $T_w - T_0 = 8$, Ar = 6.9

(g) $u_0 = 0.2$, $T_w - T_0 = 15$, Ar = 416 (h) $u_0 = 0.4$, $T_w - T_0 = 15$, Ar = 73 (i) $u_0 = 0.8$, $T_w - T_0 = 15$, Ar = 13

Fig. 3. Predicted temperature contours.

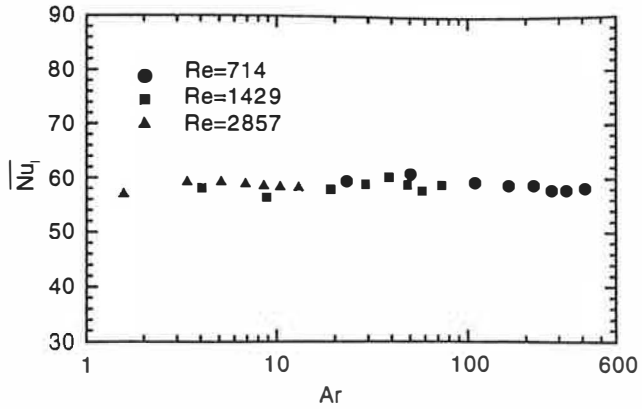

Fig. 4. Average Nusselt number along the left vertical wall.

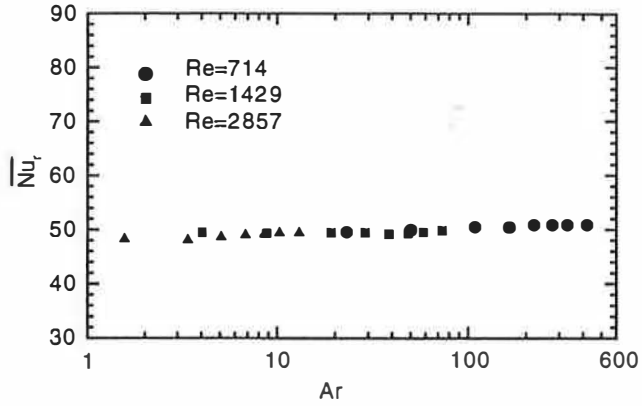

Fig. 5. Average Nusselt number along the right vertical wall.

function of both Ar and Re numbers. The disagreement between our results and Mullejan's probably lies on the different locations of supply air. In Mullejan's case, the change of supply air velocity and temperature, hence the change of Ar and Re numbers, would result in significant changes of flow pattern. But, this does not happen in our study, as shown in Fig. 2. The linear ceiling supply offers a stable flow pattern in the room over the entire practical range of air supply condition for air-conditioning.

The effect of room Archimedes number on the non-dimensional temperature ratio, θ, is studied to evaluate the effectiveness of the ventilation system on removing heat load from the room. θ is defined as

$$\theta = \frac{(T_e - T_0)}{(T_w - T_0)} \tag{20}$$

where subscript e, 0 and w refer to extract, supply and heated wall temperatures. Figure 6 plotted the non-dimensional temperature θ against Ar. The results show that θ increases with Ar constantly, which indicates that the air mixing in the room becomes more effective as Ar increases. This is due to the increase of the buoyancy effect which promotes the air mixing in the room.

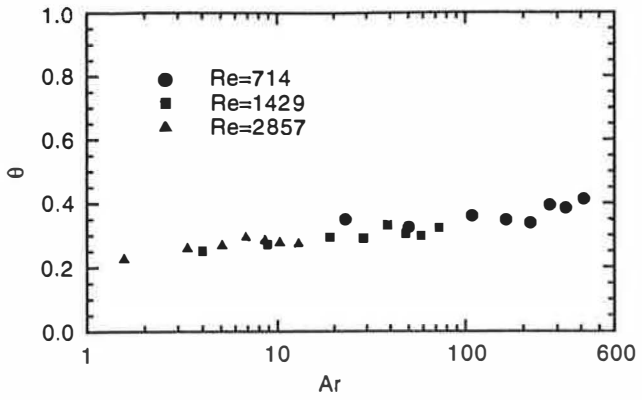

Fig. 6. Effect of Ar number on the room temperature ratio.

Figure 7 shows the contours of turbulent kinetic energy in the room. It is noticed that high level of turbulence kinetic energy (hence high turbulent mixing) is coupled with the large Ar number. The higher turbulent mixing tends to smooth out the temperature gradients. Referring back to the temperature contour in Fig. 3 (g), very uniform temperature distribution is achieved due to high local turbulent level.

At the turbulent regime, the buoyancy force does not only affect the averaged flow, but also the fluctuating flow. In order to evaluate the average turbulence level, an average turbulent kinetic energy k_a is plotted against Ar number in Fig. 8. It is found that the dimensionless turbulence kinetic energy k_a/u_0^2 increases with Ar number. When Ar number exceeds 200, a rapid increase of k_a/u_0^2 is seen. This implies an enhanced turbulence mixing induced by high buoyancy force.

5. Conclusions

High Reynolds number k–ε turbulence model was used to simulate room air motion using linear ceiling air supply configuration. Even though the selected geometry was comparatively simple, we successfully simulated the room air mixing under the complex turbulence flow and mixed convection heat transfer. The influences of different air supply velocities and temperatures on the distribution of mean room velocity, temperature and turbulence kinetic energy have been studied in detail.

A modified Archimedes number is used to characterize the air mixing behaviors for non-isothermal room ventilation flow at different convection regimes. It is found that average Nusselt numbers are little affected by Ar number and Reynolds number. But the non-dimensional temperature ratio θ and averaged turbulent kinetic energy k_a increase with Ar number.

The simulated results indicate that the linear ceiling air supply configuration with a high level air return can achieve a well-mixed air motion characteristic in a wide

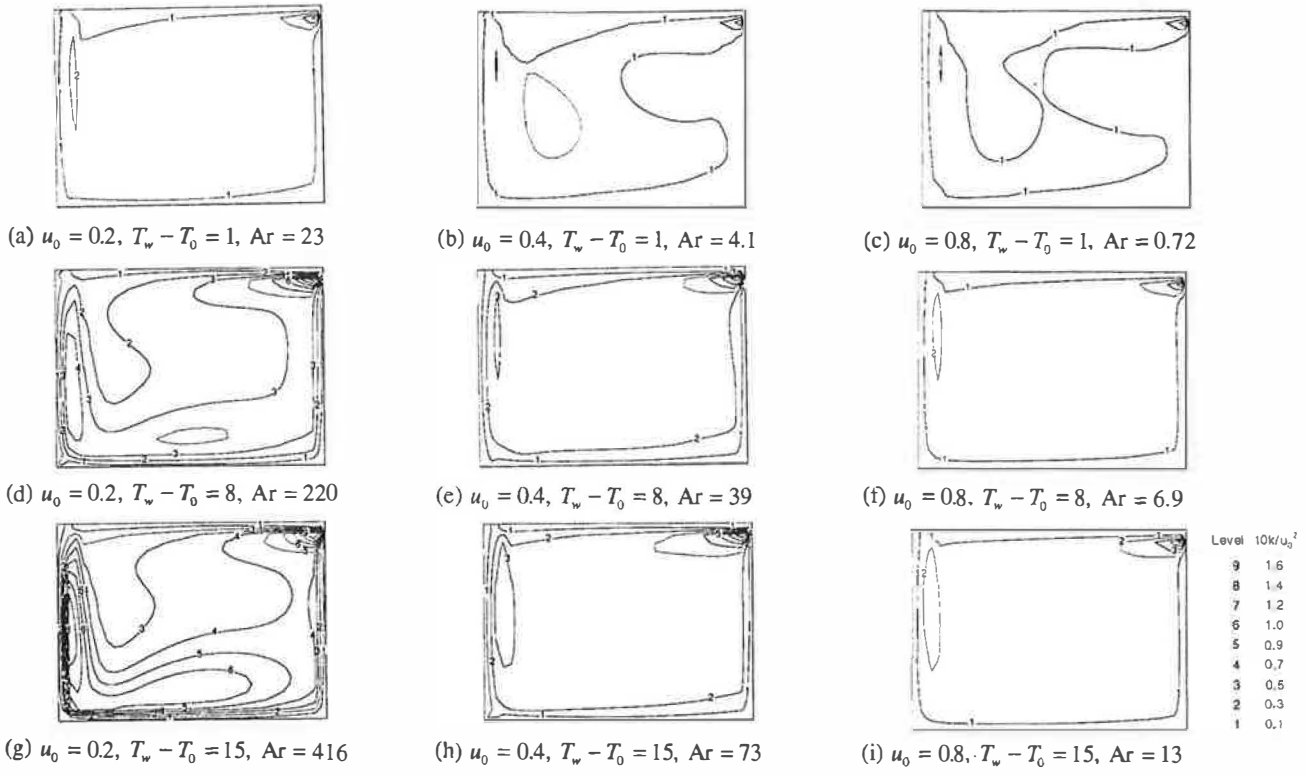

Fig. 7. Predicted turbulence kinetic energy contours.

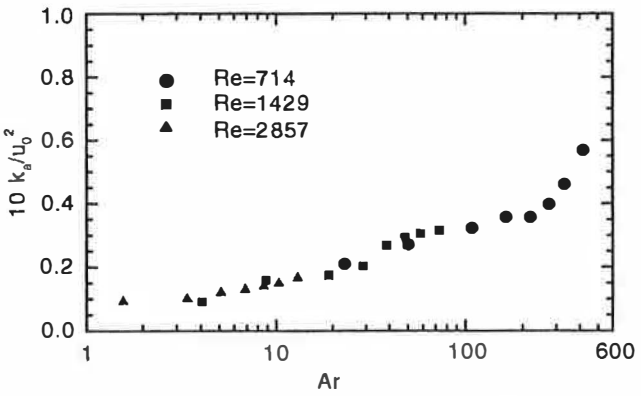

Fig. 8. Variations of $k_{a,i}/u_i^2$ with Ar number.

range of supply air velocities and temperatures. This is due to the effect of the buoyancy force which plays a role in both the averaged and fluctuating flow.

References

[1] Nielson P. V., Prediction of air flow and comfort in air conditioned spaces. ASHRAE Trans. 1975;81(2):247–53.

[2] Murakami S, Kato S. Suyama Y. Numerical and experimental study on turbulent diffusion fields in conventional flow-type clean room. ASHRAE Trans. 1989:94(2):469–93.

[3] Christianson LL. Building Systems: Room Air and Air Contaminant Distribution. ASHRAE Inc. 1989.

[4] Chow YK. Application of computational fluid dynamics in building services engineering. Building and Environment 1996;31(5):425–36.

[5] Chen, Q. Comparison of different k–ε models for indoor air flow computations. Numer. Heat Transfer Part B 1995;28:353–69.

[6] Chen, Q. Prediction of room air motion by Reynolds-stress models. Building and Environment. 1996:31(3):233–44.

[7] Rodi, W. Turbulence Models and Their Application in Hydraulics—A State of Art Review. Delft, Netherlands: Book Publication of AIHR. 1984.

[8] Patankar, SV. Numerical Heat Transfer and Fluid Flow. New York: McGraw-Hill. 1980.

[9] de Vahl Davis G. Natural convection of air in a square cavity: a bench mark numerical solution. Int. J. Numer. Meth. Fluids 1983;3:249–64.

[10] Zhang JS, Wu GJ. Christianson LL. A new similitude modeling technique for studies of non-isothermal room ventilation flows. ASHRAE Trans. 1993:99(1):129–38.

[11] Xue H, Hihara E, Saito T. Temperature stratification of heated air flow in a fire tunnel. JSME International J. Series B 1994;37(1):187–94.

[12] Muellejans. Simulation between non-isothermal flow and heat transfer in mechanically ventilated rooms. RWTH Aachen: Forschungssbericht No. 1656, 1966.